Chapter 4

Wavelets and Partial Differential Equations

4.1 Introduction: Wavelet-Galerkin Method for Partial Differential Equation

In this chapter, we will discuss the wavelet method for solving linear parabolic PDE, linear hyperbolic PDE, and based on this, we shall discuss the wavelet method for elliptic PDEs. We have discussed the general wavelet method for solving PDEs in Preface. In Section 4.2 - Section 4.7, we shall discuss the connection coefficients and the differentiability matrix with respect to the scaling function and wavelets. We have made an attempt to examine Wavelet - Galerkin method in multiresolution analysis when restricting the wavelets to a bounded domain. Finally, we have examined the computational methods and discussed some numerical examples. As discussed in Preface, the wavelet based methods for PDEs can be separated into the following classes:

- Methods based on scaling function expansions,
- Methods based on wavelet expansions,
- Wavelets and finite differences,
- Other methods.

4.2 Connection Coefficients

A natural starting point for the projection methods is the topic of two-term **connection coefficients**. We define the connection coefficients as

$$\Gamma^{d_1,d_2}_{j,l,m} = \int_{-\infty}^{\infty} \phi^{(d_1)}_{j,l}(x)\phi^{(d_2)}_{j,m}(x)dx, \quad j,l,m \in \mathbf{Z}$$

where d_1 and d_2 are orders of differentiation. We will assume for now that these derivatives are well-defined. Substituting

$$\phi_{j,k}(x) = 2^{j/2}\phi(2^j x - k),$$
$$\psi_{j,k}(x) = 2^{j/2}\psi(2^j x - k),$$

we obtain

$$\Gamma^{d_1,d_2}_{j,l,m} = \int_{-\infty}^{\infty} (2^{j/2}\phi(2^j x - l))^{(d_1)}(2^{j/2}\phi(2^j x - m))^{(d_2)}dx, \quad j,l,m \in \mathbf{Z}$$

and hence,

$$\Gamma^{d_1,d_2}_{j,l,m} = \int_{-\infty}^{\infty} 2^{j/2}\phi^{(d_1)}(2^j x - l)2^{jd_1}2^{j/2}\phi^{(d_2)}(2^j x - m)2^{jd_2}dx, \quad j,l,m \in \mathbf{Z}.$$

Using the changes of variable $x \leftarrow (2^j x - l)$, we find that

$$\Gamma^{d_1,d_2}_{j,l,m} = 2^j 2^{j(d_1+d_2)} \int_{-\infty}^{\infty} \phi^{(d_1)}(x)\phi^{(d_2)}(x - m + l)\frac{dx}{2^j}$$

and hence,

$$\begin{aligned}\Gamma^{d_1,d_2}_{j,l,m} &= 2^{jd} \int_{-\infty}^{\infty} \phi^{(d_1)}(x)\phi^{(d_2)}(x - m + l)dx \\ &= 2^{jd}\Gamma^{d_1,d_2}_{0,0,m-l}\end{aligned}$$

where $d = d_1 + d_2$. Since as the scaling functions have compact support repeated integration by parts yields the identity

$$\Gamma^{d_1,d_2}_{0,0,n} = (-1)^{d_1}\Gamma^{0,d}_{0,0,n}.$$

Thus,

$$\Gamma^{d_1,d_2}_{j,l,m} = (-1)^{d_1}2^{jd}\Gamma^{0,d}_{0,0,m-l}.$$

Therefore, it is sufficient to consider only one order of differentiation (d) and one shift parameter ($m - l$) and we define

$$\Gamma^d_l = \int_{-\infty}^{\infty} \phi(x)\phi^{(d)}_l(x)dx, l \in \mathbf{Z}. \tag{4.1}$$

Consequently

$$\Gamma^{d_1,d_2}_{j,l,m} = (-1)^{d_1} 2^{jd} \Gamma^d_{m-l} \tag{4.2}$$

Using the changes of variable $x \leftarrow x + l$ in (4.1) and $\phi_{j,k}(x) = 2^{j/2}\phi(2^j x - k)$, we obtain

$$\Gamma^d_l = \int_{-\infty}^{\infty} \phi(x+l)\phi^{(d)}(x)dx, \quad l \in \mathbf{Z}.$$

Now, repeated integration by parts yields the following property:

$$\Gamma^d_n = (-1)^d \Gamma^d_{-n}, \quad n \in [2-D, D-2]. \tag{4.3}$$

We now look into the problem of computing (4.1). The supports of ϕ and $\phi^{(d)}_l$ overlap only for $-(D-2) \leq l \leq D-2$, so there are $2D-3$ nonzero connection coefficients to be determined. Let

$$\mathbf{\Gamma}^d = \{\Gamma^d_l\}_{l=2-D}^{D-2}$$

and we assume that $\phi \in C^d(\mathbf{R})$. Then taking the identity

$$\phi_{j-1,l}(x) = \sum_{k=0}^{D-1} a_k \phi_{j,2l+k}(x)$$

with $j = 1$ and differentiating it d times leads to

$$\phi^{(d)}_l(x) = \sum_{k=0}^{D-1} a_k \phi^{(d)}_{l,2l+k}(x) = 2^d \sqrt{2} \sum_{k=0}^{D-1} a_k \phi^{(d)}_{2l+k}(2x). \tag{4.4}$$

Substituting the dilation equation

$$\phi(x) = \sqrt{2} \sum_{k=0}^{D-1} a_k \phi(2x-k)$$

and (4.4) into (4.1) yields

$$\begin{aligned}
\Gamma^d_l &= \int_{-\infty}^{\infty} \left[\sqrt{2}\sum_{r=0}^{D-1} a_r \phi_r(2x)\right] \left[2^d\sqrt{2}\sum_{s=0}^{D-1} a_s \phi^{(d)}_{2l+s}(2x)\right] dx \\
&= 2^{d-1} \sum_{r=0}^{D-1}\sum_{s=0}^{D-1} a_r a_s \int_{-\infty}^{\infty} \phi_r(2x)\phi^{(d)}_{2l+s}(2x)dx, \quad x \leftarrow 2x \\
&= 2^{d} \sum_{r=0}^{D-1}\sum_{s=0}^{D-1} a_r a_s \int_{-\infty}^{\infty} \phi_r(x)\phi^{(d)}_{2l+s}(x)dx, \quad x \leftarrow x - r \\
&= 2^{d} \sum_{r=0}^{D-1}\sum_{s=0}^{D-1} a_r a_s \int_{-\infty}^{\infty} \phi(x)\phi^{(d)}_{2l+s}(x)dx,
\end{aligned}$$

Hence,

$$\sum_{r=0}^{D-1}\sum_{s=0}^{D-1} a_r a_s \Gamma^d_{2l+s-r} = \frac{1}{2^d}\Gamma^d_l, \quad l \in [2-D, D-2]. \tag{4.5}$$

Let $n = 2l+s-r$. Since Γ^d_n is nonzero only for $n \in [2-D, D-2]$ then $s = r+n-2l$ as well as r must be restricted to $[0, D-1]$. This is fulfilled for $\max(0, 2l-n) \le r \le \min(D-2, D-2+2l-n)$. Let $p = 2l-n$ and define

$$\bar{a}_p = \sum_{r=r_1(p)}^{r_2(p)} a_r a_{r-p}$$

where $r_1(p) = \max(0,p)$ and $r_2(p) = \min(D-1, D-1+p)$. Hence (4.5) becomes

$$\sum_{n=2-D}^{D-2} \bar{a}_{2l-n}\Gamma^d_n = \frac{1}{2^d}\Gamma^d_l, \quad l \in [2-D, D-2].$$

In the matrix-vector, from this relation becomes

$$(\mathbf{A} - 2^{-d}\mathbf{I})\mathbf{\Gamma}^d = 0, \tag{4.6}$$

where $\mathbf{A}$ is a $(2D-3)\times(2D-3)$ matrix with the elements

$$[\mathbf{A}]_{l,n} = \bar{a}_{2l-n}, \quad l, n \in [2-D, D-2].$$

Properties of $\bar{a}$:

- Because of the orthogonality property $\sum_{k=0}^{D-1} a_k a_{k+2n} = \delta_{0,n}, \quad n \in \mathbf{Z}$, we obtain

$$\bar{a}_p = \begin{cases} 1, & for \quad p = 0 \\ 0, & for \quad p = \pm 2, \pm 4, \pm 6, ... \end{cases}$$

- Since, $\bar{a}_p = \bar{a}_{-p}$ so we need only to compute $\bar{a}_p$ for $p > 0$.
- As a consequence of one of the properties of filter coefficients i.e,

$$\sum_{l=0}^{D/2-l}\sum_{n=0}^{D-2l-2} a_n a_{n+2l+1} = \frac{1}{2}$$

  we obtain

$$\sum_{p \text{ odd}} \bar{a}_p = 1.$$

Hence all columns add to one, which means that $\mathbf{A}$ has the left eigenvector $[1, 1, ...1]$ corresponding to the eigenvalue $1, d = 0$ in (4.6). Consequently, $\mathbf{A}$ has the structure shown here for $D = 6$:

$$\begin{pmatrix}
0 & \bar{a}_5 & & & & & & & \\
0 & \bar{a}_3 & 0 & \bar{a}_5 & & & & & \\
1 & \bar{a}_1 & 0 & \bar{a}_3 & 0 & \bar{a}_5 & & & \\
0 & \bar{a}_1 & 1 & \bar{a}_1 & 0 & \bar{a}_3 & 0 & \bar{a}_5 & \\
0 & \bar{a}_3 & 0 & \bar{a}_1 & 1 & \bar{a}_1 & 0 & \bar{a}_3 & 0 \\
 & \bar{a}_5 & 0 & \bar{a}_3 & 0 & \bar{a}_1 & 1 & \bar{a}_1 & 0 \\
 & & & \bar{a}_5 & 0 & \bar{a}_3 & 0 & \bar{a}_1 & 1 \\
 & & & & & \bar{a}_5 & 0 & \bar{a}_3 & 0 \\
 & & & & & & & \bar{a}_5 & 0
\end{pmatrix}.$$

Equation (4.6) has a non-trivial solution if 2^{-d} is an eigenvalue of $\mathbf{A}$. Numerical calculations for $D = 4, 6, \cdots, 30$ indicate that 2^{-d} is an eigenvalue for $d = 0, 1, \cdots, D-1$ and that dimension of each corresponding eigen space is 1. Hence, one additional equation is needed to normalize the solution.

To this end, we have used the property of vanishing moments. Recall that $P = \frac{D}{2}$. Assuming that $d < P$, we obtain from the equation:

$$x^p = \sum_{k=-\infty}^{\infty} M_k^p \phi(x-k), \quad x \in \mathbf{R}, \quad p = 0, 1, \cdots, P-1,$$

where

$$M_k^p = \int_{\infty}^{\infty} x^p \phi(x-k)dx, \quad k \in \mathbf{Z}, \quad p = 0, 1, \cdots, P-1,$$

that

$$x^d = \sum_{l=-\infty}^{\infty} M_l^d \phi(x-l).$$

Differentiating both sides of this relation d times yields

$$d! = \sum_{l=-\infty}^{\infty} M_l^d \phi^{(d)}(x-l).$$

Multiplying by $\phi(x)$ and integrating, we then find that

$$\begin{aligned}
d! \int_{\infty}^{\infty} \phi(x) &= \sum_{l=-\infty}^{\infty} M_l^d \int_{\infty}^{\infty} \phi(x)\phi^{(d)}(x-l)dx \\
&= \sum_{l=2-D}^{D-2} M_l^d \int_{\infty}^{\infty} \phi(x)\phi^{(d)}(x-l)dx
\end{aligned}$$

Hence, we obtain

$$\sum_{l=2-D}^{D-2} M_l^d \Gamma_l^d = d! \tag{4.7}$$

which closes the system (4.6). The computation of the moments needed for this equation is described in Appendix A. $\mathbf{\Gamma}^d$ is then found as follows:
Let v^d be an eigenvector corresponding to the eigenvalue 2^{-d} in (4.6). Then $\mathbf{\Gamma}^d = kv^d$ for some constant k, which is fixed according to (4.7).

Remark 4.2.1 *There is one exception to the statement that 2^{-d} is an eigenvalue of $\mathbf{A}$ for $d = 0, 1, \cdots, D-1$. Let $D = 4$ then the eigenvalues of $\mathbf{A}$ are*

$$\frac{1}{8}, \frac{1}{4} + 6.4765 \times 10^{-9}i, \frac{1}{4} + 6.4765 \times 10^{-9}i, \frac{1}{2}, 1.$$

Consequently, $\frac{1}{4}$ is not an eigenvalue of A and connection coefficients for the combination $D = 4, d = 2$ are not well defined.

4.3 Differentiability

The question of differentiability of ϕ (and hence ψ) is non-trivial and not fully understood (see [SN96]). However, some basic results are given in [Eir92] and shown in Table-4.1. The space

D	2	4	6	8	10	12	14	16	18	20
α	-	0	1	1	1	1	2	2	2	2
β	0	0	1	1	2	2	2	2	3	3

Table 4.1: **Regularity of Scaling functions and Wavelets.**

$C^{\alpha}(\mathbf{R})$ denotes the space of functions having continuous derivative of order $\leq \alpha$. The space $H^{\beta}(\mathbf{R})$ is a Sobolev space defined as

$$H^{\beta}(\mathbf{R}) = \{f \in L^2(\mathbf{R}) : f^{(d)} \in L^2(\mathbf{R}), \;\; |d| \leq \beta\}.$$

This latter concept is a generalization of ordinary differentiability, hence $\alpha \leq \beta$.

4.4 Differentiation Matrix with respect to Scaling Functions

Let f be a function in $V_J \bigcap C^d(\mathbf{R}), J \in N_0$. The connection coefficients described earlier can be used to evaluate the d^{th} order derivative of f in terms of its scaling function coefficients. Differentiating both sides of the equation

$$f(x) = \sum_{t=-\infty}^{\infty} c_{J,l}\phi_{J,l}(x), \quad x \in \mathbf{R}$$

d times, where

$$c_{J,l} = \int_{-\infty}^{\infty} f(x)\phi_{J,l}(x)dx$$

we obtain

$$f^{(d)}(x) = \sum_{l=-\infty}^{\infty} c_{J,l}\phi_{J,l}^{(d)}(x), \quad x \in \mathbf{R}. \tag{4.8}$$

$f^{(d)}$, in general, may not belong to V_J, so we now project $f^{(d)}$ back onto V_J via

$$(P_{V_J}f^{(d)})(x) = \sum_{k=-\infty}^{\infty} c_{J,l}^{(d)}\phi_{J,k}(x), \quad x \in \mathbf{R} \tag{4.9}$$

where, according to the equation:

$$c_{J,l} = \int_{-\infty}^{\infty} f(x)\phi_{J,l}(x)dx$$

we obtain,

$$c_{J,k}^{(d)} = \int_{-\infty}^{\infty} f^{(d)}(x)\phi_{J,k}(x)dx \tag{4.10}$$

So, we have

$$\begin{aligned}
c_{J,k}^{(d)} &= \sum_{l=-\infty}^{\infty} c_{J,l} \int_{-\infty}^{\infty} \phi_{J,k}(x)\phi_{J,l}^{(d)}(x)dx \\
&= \sum_{l=-\infty}^{\infty} c_{J,l}\Gamma_{J,k,l}^{0,d} \\
&= \sum_{l=-\infty}^{\infty} c_{J,l}2^{Jd}\Gamma_{l-k}^{d} \\
&= \sum_{n=-\infty}^{\infty} c_{J,n+k}2^{Jd}\Gamma_{n}^{d}, \quad -\infty < k < \infty
\end{aligned}$$

We used (4.2) for the second last equality. Since Γ^d_n is only nonzero for $n \in [2-D, D-2]$, we find that

$$c^{(d)}_{J,k} = \sum_{n=2-D}^{D-2} c_{J,n+k} 2^{Jd} \Gamma^d_n, \quad J, k \in \mathbf{Z}. \tag{4.11}$$

If f is 1-periodic, then

$$c_{J,l} = c_{J,l+p2^J}, \quad l, p \in \mathbf{Z}$$

and

$$c^{(d)}_{j,K} = c^{(d)}_{j,k+p2^J}, \quad k, p \in \mathbf{Z}.$$

Hence, it is sufficient to consider 2^J coefficients of either type. Therefore,

$$c^{(d)}_{J,k} = \sum_{n=2-D}^{D-2} c_{J,\langle n+k\rangle_{2}^{Jd}} \Gamma^d_n \tag{4.12}$$

$$k = 0, 1, \cdots, 2^J - 1.$$

. This system of equation can be represented in matrix-vector form

$$\mathbf{c}^{(d)} = \mathbf{D}^{(d)} \mathbf{c}, \tag{4.13}$$

where

$$\left[\mathbf{D}^d\right]_{k,\langle n+k\rangle_{2^J}} = 2^{Jd} \Gamma^d_n,$$

$$k = 0, 1, \cdots, 2^J - 1,$$

$$n = 2-D, 3-D, \cdots, D-2$$

and

$$\mathbf{c}^{(d)} = \left[c^{(d)}_{J,0}, c^{(d)}_{J,1}, \cdots, c^{(d)}_{J,2^J-1}\right].$$

We shall refer to the matrix $\mathbf{D}^{(d)}$ as the **Differentiation Matrix of order d**. $\mathbf{D}^{(d)}$ is symmetric for d even and skew-symmetric for d odd. It also follows that $\mathbf{D}^{(d)}$ is circulant. Also, the bandwidth of the differentiation matrix is $2D-3$. The differentiation matrix has the following structure (shown for $D = 4$, and $J = 3$):

$$\mathbf{D}^{(d)} = 2^3 \begin{pmatrix} \Gamma^d_0 & \Gamma^d_1 & \Gamma^d_2 & 0 & 0 & 0 & (-1)^d\Gamma^d_2 & (-1)^d\Gamma^d_1 \\ (-1)^d\Gamma^d_1 & \Gamma^d_0 & \Gamma^d_1 & \Gamma^d_2 & 0 & 0 & 0 & (-1)^d\Gamma^d_2 \\ (-1)^d\Gamma^d_2 & (-1)^d\Gamma^d_1 & \Gamma^d_0 & \Gamma^d_1 & \Gamma^d_2 & 0 & 0 & 0 \\ 0 & (-1)^d\Gamma^d_2 & (-1)^d\Gamma^d_1 & \Gamma^d_0 & \Gamma^d_1 & \Gamma^d_2 & 0 & 0 \\ 0 & 0 & (-1)^d\Gamma^d_2 & (-1)^d\Gamma^d_1 & \Gamma^d_0 & \Gamma^d_1 & \Gamma^d_2 & 0 \\ 0 & 0 & 0 & (-1)^d\Gamma^d_2 & (-1)^d\Gamma^d_1 & \Gamma^d_0 & \Gamma^d_1 & \Gamma^d_2 \\ \Gamma^d_2 & 0 & 0 & 0 & (-1)^d\Gamma^d_2 & (-1)^d\Gamma^d_1 & \Gamma^d_0 & \Gamma^d_1 \\ \Gamma^d_1 & \Gamma^d_2 & 0 & 0 & 0 & (-1)^d\Gamma^d_2 & (-1)^d\Gamma^d_1 & \Gamma^d_0 \end{pmatrix}$$

A special case is $d = 1$ and define

$$\mathbf{D} = \mathbf{D}^{(1)}. \tag{4.14}$$

4.5 Differentiation Matrix with respect to Physical Space

We shall restrict our attention to the periodic case only. However, the non-periodic case can be considered in a similar manner. Note that

$$\mathbf{f} = \mathbf{Tc}, \quad i.e. \quad \mathbf{c} = \mathbf{T}^{-1}\mathbf{f},$$

where $\mathbf{f}$ are the grid values of a function $f \in \tilde{V}_J$ defined on the unit interval. $\mathbf{c}$ is the vector of scaling function coefficients corresponding to $\mathbf{f}$. Similarly, the projection of $\mathbf{f}^{(\mathbf{d})}$ onto $\tilde{V}_J$ satisfies

$$\mathbf{f}^{(\mathbf{d})} = \mathbf{Tc}^{(\mathbf{d})},$$

and hence, we get

$$\mathbf{f}^{(\mathbf{d})} = \mathbf{TD}^{(\mathbf{d})}\mathbf{T}^{-1}\mathbf{f}.$$

We call $\mathbf{D}^{(\mathbf{d})}$ the differentiation matrix with respect to the coefficient space, and $\mathbf{TD}^{(\mathbf{d})}\mathbf{T}^{-1}$ the differentiation matrix with respect to physical space. The matrix $\mathbf{T}$ and $\mathbf{D}^{(d)}$ are both circulant with the same dimensions $(2D-3) \times (2D-3)$, so they are diagonalized by the same matrix, namely, the Fourier matrix $\mathbf{F}_{2D-3}$. Therefore, they commute according to Theorem A.3.5 of Appendix A and we find that

$$\mathbf{TD}^{(d)}\mathbf{T}^{-1} = \mathbf{D}^{(d)}\mathbf{TT}^{-1} = \mathbf{D}^{(d)}$$

and

$$\mathbf{f}^{(d)} = \mathbf{D}^{(d)}\mathbf{f}. \tag{4.15}$$

Hence, $\mathbf{D}^{(d)}$ is the differentiation matrix with respect to both coefficient space and physical space.

4.6 Differentiation Matrix for Functions with Period L

If the function to be differentiated is periodic with period L, i.e.,

$$f(x) = f(x+L), x \in \mathbf{R}$$

then we can map one period to the unit interval and apply the various transform matrices. Thus, let $y = x/L$ and define

$$g(y) \equiv f(Ly) = f(x)$$

then g is 1-periodic and we define the vector

$$\mathbf{g} = [g_0, g_1, \cdots, g_{2^J-1}]$$

by

$$g_k = (P_{\tilde{V}_J} g)(k/2^J); \quad k = 0, 1, \cdots, 2^J - 1.$$

Let $\mathbf{f} = \mathbf{g}$. Then $\mathbf{f}$ approximates $f(x)$ at $x = kL/2^J$. We have

$$\mathbf{g}^{(d)} = \mathbf{D}^{(d)} \mathbf{g}.$$

Hence, by chain rule

$$f^{(d)}(x) = \frac{1}{L^d} g^{(d)}(y).$$

Therefore, we have

$$\mathbf{f}^{(d)}(x) = \frac{1}{\mathbf{L}^d} \mathbf{g}^{(d)} = \frac{1}{\mathbf{L}^d} \mathbf{D}^{(d)} \mathbf{g} = \frac{1}{\mathbf{L}^d} \mathbf{D}^{(d)} \mathbf{f}. \tag{4.16}$$

4.7 Differentiation Matrix with respect to Wavelet Space

Let f be a function in $\tilde{V}_J$ and hence,

$$f(x) = \sum_{l=0}^{2^{J_0}-1} c_{J_0,l} \tilde{\phi}_{J_0,l}(x) + \sum_{j=J_0}^{J-1} \sum_{l=0}^{2^j-1} d_{j,l} \tilde{\psi}_{j,l}(x), \quad x \in [0, 1]. \tag{4.17}$$

We now, differentiate both sides of the above equation d times to obtain

$$f^{(d)}(x) = \sum_{l=0}^{2^{J_0}-1} c_{J_0,l} \tilde{\phi}^{(d)}_{J_0,l}(x) + \sum_{j=J_0}^{J-1} \sum_{l=0}^{2^j-1} d_{j,l} \tilde{\psi}^{(d)}_{j,l}(x).$$

Projecting $f^{(d)}$ onto $\tilde{V}_J$ yields

$$\left(P_{V_J} f^{(d)}\right)(x) = \sum_{l=0}^{2^{J_0}-1} c^{(d)}_{J_0,l} \tilde{\phi}_{J_0,l}(x)$$

$$+ \sum_{j=J_0}^{J-1} \sum_{l=0}^{2^j-1} d^{(d)}_{j,l} \tilde{\psi}_{j,l}(x),$$

where

$$\begin{aligned} c_{J_0,l}^{(d)} &= \int_{-\infty}^{\infty} f^{(d)}(x)\tilde{\phi}_{J_0,l}(x)dx, \quad l = 0, 1, \cdots, 2^{J_0} - 1 \\ d_{j,l}^{(d)} &= \int_{-\infty}^{\infty} f^{(d)}(x)\tilde{\psi}_{j,l}(x)dx, j = J_0, J_0+1, \cdots, J-1. \end{aligned} \tag{4.18}$$

Given the scaling function coefficient of $f^{(d)}$ on the finest level, we can use the FWT to obtain the wavelet coefficient above. Hence,

$$\mathbf{d}^{(d)} = \mathbf{W}\mathbf{c}^{(d)}$$

where $\mathbf{c}^{(d)}$ is defined as in Section 4.5 and $\mathbf{d}^{(d)}$ contains the coefficients in (4.18). Using (4.13) and $\mathbf{x} = \left(\mathbf{W}^{\lambda}\right)^T \breve{\mathbf{x}}$, we obtain

$$\mathbf{d}^{(d)} = \mathbf{W}\mathbf{D}^{(d)}\mathbf{c} = \mathbf{W}\mathbf{D}^{(d)}\mathbf{W}^T\mathbf{d}$$

or

$$\mathbf{d}^{(d)} = \breve{\mathbf{D}}^{(d)}\mathbf{d} \tag{4.19}$$

where we have defined

$$\breve{\mathbf{D}}^{(d)} = \mathbf{W}\mathbf{D}^{(d)}\mathbf{W}^T.$$

4.8 Wavelet-Galerkin Method for Second Order Wave Equation

Now, we shall discuss the wavelet method for solving linear hyperbolic boundary value problems. We examine Wavelet-Galerkin method in the multiresolution analysis when restricting the wavelets to a bounded domain. Semi-discrete Wavelet-Galerkin method is discussed with related error analysis. Finally, we have examined computational methods and numerical example. Consider the following second order wave equation ($1D$):

$$u_{tt} - u_{xx} + \lambda u = f(x,t), \quad x \in \Omega = (0,1), \quad t > 0, \quad \lambda > 0. \tag{4.20}$$

Initial Conditions are

$$u(x,0) = u_0(x)$$

$$u_t(x,0) = u_1(x), \quad x \in \Omega,$$

and Boundary Conditions are

$$u(0,t) = u(1,t) = 0, \quad t \in R.$$

Assume that f, u_0, u_1 are given functions. Let $V = H_0^1(\Omega)$, where

$$H_0^1(\Omega) = \{v \in H^1(\Omega) : v(x) = 0, x \in \Omega\}.$$

4.8.1 Weak Formulation

For the weak formulation: Multiply (4.20) by $v \in H_0^1$ and integrate by parts to obtain as follows: Find $u(\cdot, t) \in V = H_0^1(\Omega)$ such that for $t > o$

$$\begin{aligned} (u_{tt}, v) + a(u, v) &= (f, v), \quad v \in H_0^1, \\ (u(0), v) &= (u_0, v), \\ (u_t(0), v) &= (u_1, v), \end{aligned} \tag{4.21}$$

where

$$a(u, v) = \int_0^1 (u_x v_x dx) + \lambda \int_0^1 u(x) v(x) dx.$$

Note that $a(\cdot, \cdot)$ satisfy the coercivity and boundedness property. Using Cauchy-Schwartz inequality, Holder's inequality, Poincare's inequality and the definition of H_1 norm , we find that $a(\cdot, \cdot)$ is bounded which is shown as follows:

$$\begin{aligned} |a(\phi, \psi)| &\leq \int_0^1 |\phi_x||\psi_x| dx + |\lambda| \int_0^1 |\phi(x)||\psi(x)| dx \\ &\leq M \left(\int_0^1 |\phi_x||\psi_x| dx + \int_0^1 |\phi(x)||\psi(x)| dx \right) \\ &\leq M \|\phi\|_1 \|\psi\|_1. \end{aligned}$$

For coercive of $a(\cdot, \cdot)$, we use the fact that $\lambda > 0$

$$\begin{aligned} \|a(\phi, \phi)\| &= \int_0^1 |\phi_x|^2 + \int_0^1 |\phi(x)|^2 dx \\ &\geq \alpha \int_0^1 \left(|\phi(x)|^2 + |\phi(x)|^2 \right) dx \\ &\geq \alpha \|u(x)\|_1 \end{aligned}$$

where, $\alpha = \min(1, \lambda)$. We also have the following theorem:

Theorem 4.8.1 *Let $P_j : L^2(0,1) \to V_j(0,1)$ be the L^2 projection. Then $\forall r \leq s, 0 \leq r \leq R, 0 \leq s \leq P+1, f \in H^s(0,1)$ implies*

$$\|f - P_j f\|_{H^r(0,1)} \leq 2^{-j(s-r)} \|f^(s)\|_{L^2(0,1)}.$$

Proof: For $r = 0$,

$$\|f - P_j f\|_{L^2(0,1)} \leq 2^{-js} \|f^(s)\|_{L^2(0,1)} r = 0, 1.$$

has been proved in Chapter 2, in Subsection 2.11.2. Now, in order to estimate $\|f - P_j f\|_{H^r(0,1)}$, we replace f by f' (the first derivative of f w.r.t x) in the Theorem 1.4.2 and proceed as in the approximation properties of $\tilde{V}_j$ in Subsection 2.11.2. Hence, we obtain the proof of this lemma.

4.8.2 Wavelet-Galerkin Method to solve Hyperbolic Equation

In a Galerkin type approach, we first introduce the space of functions in V_j satisfying the boundary conditions,

$$V_j^0 = \{u \in V_j(0,1)|u(0) = u(1) = 0\}.$$

Wavelet-Galerkin method is to find $u_j(t) \in V_j^0, t \geq 0$ such that

$$(u_{jtt}, v_j) + a(u_j, v_j) = (f, v_j), \quad v_j \in V_j^0,$$

with initial condition

$$(u(0), v_j) = (u_0, v_j).$$

4.8.3 Semi-Discrete Wavelet-Galerkin Method

Let V_J be a finite dimensional subspace of $V = H_0^1(\Omega)$ i.e. $V_J \subset V$ satisfied the following approximation properties

$$\inf_{\chi \in V_h} \left\{\|v - \chi\| + 2^{-J}\|v - \chi\|_1\right\} \leq C^{2^{-Jr}}\|v\|_r,$$

$$\forall v \in H^r(\Omega) \cap V, \quad r \leq P,$$

where $P=$ number of vanishing moments. In the semi-discrete Galerkin approximation, we seek $u_J(t) \in V_J^0$ such that for $t > 0$

$$(u_{Jtt}, \chi) + a(u_j, \chi) = (f, \chi), \chi \in V_J^0, \tag{4.22}$$

$$(u_J(0), \chi) = (u_0, \chi), \chi \in V_J^0,$$

$$(u_J(0), \chi) = (u_0, \chi), \chi \in V_J^0$$

that is $u_J(0)$ and $u_{Jt}(0)$ are approximation of u_0 and u_1, respectively in V_J^0.

4.8.4 Error Analysis for the Semi-Discrete Method

A direct comparison between u and u_J does not yield optimal order of convergence. Therefore, we need to introduce an auxiliary function $\tilde{u}_J \in V_J^0$ which is defined by

$$a(u - \tilde{u}_J, \chi) = 0, \chi \in V_J^0. \tag{4.23}$$

Lemma 4.8.2 *Let $u - \tilde{u}_J = \eta$. Then the following estimate holds:*

$$\|\eta\|_{L^2} + 2^{-J}\|\eta\|_1 \leq C2^{-Jr}\|u\|_r,$$

and

$$\sum_{l=0}^{2}\left(\left\|\frac{\partial^l \eta}{\partial t^l}\right\| + 2^{-J}\left\|\frac{\partial^l \eta}{\partial t^l}\right\|\right) \leq C2^{-Jr}\sum_{l=0}^{2}\left\|\frac{\partial^l u}{\partial t^l}\right\|_r.$$

Proof: By the coercivity property of $a(.,.)$, we have

$$\begin{aligned}\alpha_0\|u - \tilde{u}_j\|_1^2 &\leq a(u - \tilde{u}_j, u - \tilde{u}_j)\\ &= a(u - \tilde{u}_j, u - u - \tilde{u}_j)\\ &= a(u - \tilde{u}_J, u - P_J - \tilde{u}_J) + a(u - \tilde{u}_J, P_J(u) - \tilde{u}_J)\end{aligned}$$

Since $P_J u - \tilde{u}_J \in V_J$ it follows from (4.23) that

$$a(u - \tilde{u}_J, P_J(u) - \tilde{u}_J) = 0$$

Note that

$$\begin{aligned}\alpha_0\|u - \tilde{u}_j\|_1^2 &\leq a(u - \tilde{u}_j, u - P_J u)\\ &\leq M\|u - \tilde{u}_J\|\|u - P_J u\|_1\end{aligned}$$

and hence using Theorem 4.8.1, we obtain

$$\begin{aligned}\|u - \tilde{u}_j\|_1 &\leq \frac{M}{\alpha_0}\|u - P_{Ju}\|_1\\ &\leq C2^{-J}(r-1)\|u\|_r\end{aligned}$$

By Aubin-Nitsche Duality, we have

$$\begin{aligned}\|u - \tilde{u}_j\| &\leq C2^{-j}\|u - \tilde{u}_j\|_1\\ \Rightarrow \|\eta\|_L^2 &\leq C2^{-j}\|\eta\|_1\\ &\leq C2^{-jr}\|u\|_r\end{aligned}$$

Hence, we obtain

$$\|\eta\|_L^2 + 2^{-j}\|\eta\|_1 \leq C2^{-jr}\|u\|_r \tag{4.24}$$

Differentiating (4.23) with respect to time twice, we obtain

$$a(\eta_{tt}, X) = 0, X \in V_j$$

Therefore, proceeding in the same manner as in the estimate of η, we can obtain the required estimate for η_{tt}. This completes the proof.

Now, let $e = u - u_j$. Using $\tilde{u}_j$, split e as

$$e = u - u_j = (u - \tilde{u}_j) - (u_j - \tilde{u}_j) = \eta - \theta$$

where

$$\eta = (u - \tilde{u}_j)$$

and

$$\theta = (u_j - \tilde{u}_j)$$

Since the estimate of $\eta_t t$ is known from Lemma 4.8.2, it is enough to estimate θ.

Using Weak formulation (4.21) and (4.23), the equation in θ

$$\begin{aligned}(\theta_{tt}, \chi) + a(\theta, \chi) &= (u_{Jtt}, \chi) + a(u_J, \chi) - (\tilde{u}_{jtt}, \chi) - a(u_J, \chi) \\ (\theta_{tt}, \chi) + a(\theta, \chi) &= (\eta_{tt}, \chi)\end{aligned} \tag{4.25}$$

Theorem 4.8.3 *Let u and u_j respectively be the solution of (4.21) and (4.22). Let $u_j(0) = \tilde{u}_j(0)$ so that $\theta(0) = 0$. Then there is a constant C independent of J such that*

$$\|e(t)\| + 2^{-J}\|e(t)\|_1 \leq C2^{-Jr}\left(\|u_1\|_r + \|u_0\|_r + \int_0^t \|u_{tt}(s)\|_r ds\right).$$

Now, taking $\chi = \theta_t$ in (4.25), we obtain

$$(\theta_t t, \theta_t) + a(\theta, \theta_t) = (\eta_t t, \theta_t)$$

$$\frac{d}{dt}(\theta, \theta) = a(\theta_t, \theta) + a(\theta, \theta_t)$$

Since $a(.,.)$ is symmetric, we have

$$\frac{1}{2}\frac{d}{dt}(\|\theta_t(t)\|^2 + a(\theta, \theta)) = (\eta_t t, \theta_t) \leq \|\eta_t t\|\|\theta_t\|.$$

The last inequality is obtained by Cauchy-Schwartz inequality. Define the energy norm as

$$E_\theta^2(t) = \|\theta_t(t)\|^2 + a(\theta(t), \theta(t))$$

$$fracddtE_\theta^2(t) \leq 2\|\eta_t t\|\|E_\theta(t)\| \tag{4.26}$$

Set for $t^* \in [0, t]$ such that

$$E_\theta(t^*) = \max_{0 \leq s \leq t} E_\theta(t)$$

Integrating (4.26) from 0 to t, we obtain

$$E_\theta^2(t) \leq E_\theta^2(0) + 2\int_0^t \|\eta_t t\| \|E_\theta(s)ds\| \tag{4.27}$$

Since (4.27) is true for $t = T^*$, we obtain from (4.27)

$$E_\theta^2(t^*) \leq E_\theta^2(0) + 2\int_0^{t^*} \|\eta_{tt}(s)\| \|E_\theta(s)ds\|$$

and hence

$$E_\theta^2(t^*) \leq (E_\theta(0) + 2\int_0^{t^*} \|\eta_{tt}(s)\|ds)\|E_\theta(t^*)\|$$

Now,

$$\begin{aligned} E_\theta(t) &\leq E_\theta(t^*) \\ &\leq E_\theta(0) + 2\int_0^{t^*} \|\eta_{tt}(s)\|ds \\ &\leq E_\theta(0) + 2\int_0^{t} \|\eta_{tt}(s)\|ds \end{aligned}$$

Therefore,

$$\|\theta_t(t)\|^2 + a(\theta(t),\theta(t))^{1/2} \leq \left(\|\theta_t(0)\|^2 + a(\theta(0),\theta(0))^{1/2} + C2^{-Jr}\int_0^t \|u_+tt(s)\|_r ds\right)$$

$$\begin{aligned} \|\theta_t(t)\| &\leq \|\theta_t(t)\|^2 + a(\theta(0),\theta(0))^{1/2} \\ &\leq \|\theta_t(0)\|^2 + a(\theta(0),\theta(0))^{1/2} + C2^{-Jr}\int_0^t \|u_{tt}(s)\|_r ds \end{aligned}$$

Choose $u_{Jt}(0) = P_J u_1$, then

$$\begin{aligned} \|\theta_t(0)\| &\leq \|u_{Jt}(0) - u_t(0)\| + \|u_t(0) - \tilde{u}_{Jt}(0)\| \\ &\leq C2^{-Jr}\|u_1\|_r \end{aligned}$$

Since $u_J(0) = \tilde{u}_J(0)$, $\theta(0) = 0$

$$\begin{aligned} &\sqrt{\alpha_0}\|\theta(t)\|_{H_0^1} \\ &\qquad \leq (a(\theta(t),\theta(t))^{1/2}); \quad (\textit{bycoercivity}) \\ &\qquad \leq C2^{-Jr}(\|u_1\|_r + \int_0^t \|u_{tt}(s)\|_r ds) \\ \Rightarrow \|\theta(t)\|_1 &\leq C2^{-Jr}(\|u_1\|_r + \int_0^t \|u_{tt}(s)\|_r ds) \end{aligned}$$

Therefore, the error estimate of θ in H^1-norm is

$$\|\theta(t)\|_1 \leq C2^{-Jr}(\|u_1\|_r + \int_0^t \|u_{tt}(s)\|_r ds) \tag{4.28}$$

Since $\|\theta\|_{L^2} \leq \|\theta\|_1$, we obtain an L^2-estimate for θ. Using triangle inequality and Lemma 4.8.2, we obtain the required estimate.

Remark 4.8.1 *The problem (4.20) with periodic boundary condition*

$$u(x,t) = u(x+1,t)$$

has an analogous weak formulation and error estimates as in the non periodic boundary condition with

$$V = \tilde{H}(I) = v \in H^1 : v(x+1) = v(x), x \in I.$$

4.8.5 Computational Results for the Wave Equation

We shall solve the wave equation using wavelets. We assume that the boundary condition are periodic and make use of the periodized wavelets mentioned in the earlier chapters. We begin by considering a **periodic boundary value problem**. We now consider the periodic initial-value problem for the second order wave equation $(1D)$

$$u_{tt} - u_{xx} = f(x), t > 0 \tag{4.29}$$

$$u(x,0) = u_0$$

$$u_t(x,0) = u_1$$

$$u(x,t) = u(x+1,t), \quad t \geq 0$$

where

$$f(x) = f(x+1), \quad u_0(x) = u_0(x+1), \quad and \quad u_1(x) = u_1(x+1).$$

We now reduce the second order wave equation into two first order ordinary differential equations as

$$u_t = v$$

and

$$v_t = D^{(2)}u + f.$$

4.8.6 Representation with respect to Scaling Functions

We consider first the Galerkin method for (4.29). Now,

$$u_J(x,t) = \sum_{k=0}^{2^J-1} (c_u)_{J,k}(t)\tilde{\phi}_{J,k}(x) \tag{4.30}$$

The Galerkin discretization of (4.29)

$$\frac{d}{dt}c_u(t) = c_v(t); \tag{4.31}$$

$$\frac{d}{dt}c_v(t) = D^{(2)}c_u(t) + c_f; \quad t > 0; \tag{4.32}$$

$$c_u(0) = c_h;$$

$$c_v(0) = c_g;$$

where

$$(c_f)_{J,l} = \int_0^1 f(x)\tilde{\phi}_{J,l}(x)dx,$$

$$(c_h)_{J,l} = \int_0^1 h(x)\tilde{\phi}_{J,l}(x)dx;$$

$$(c_g)_{J,l} = \int_0^1 g(x)\tilde{\phi}_{J,l}(x)dx, \quad l = 0, 1, \cdots, 2^J - 1.$$

4.8.7 Representation with respect to Wavelets

Multiplying (4.31) and (4.32) from the left by W and inserting the identity $W^T W = I$ yields

$$\frac{d}{dt}Wc_u(t) = Wc_v(t)$$

$$\frac{d}{dt}Wc_v(t) = WD^{(2)}W^T Wc_u(t) + W_{c_f}, \quad t > 0$$

From the identities

$$d_u(t) = Wc_u(t)$$

$$d_f(t) = Wc_f(t)$$

$$\breve{D}^{(2)} = WD^{(2)}W^T.$$

We then obtain

$$\frac{d}{dt}d_u(t) = d_v(t) \tag{4.33}$$

$$\frac{d}{dt}d_v(t) = \breve{D}^{(2)}d_u(t) + d_f, \quad t > 0 \tag{4.34}$$

with the initial condition

$$d_u(0) = Wc_h$$

$$d_v(0) = Wc_g.$$

4.8.8 Representation with respect to Physical Space

Multiplying (4.31) and (4.32) from the left by T and proceeding as above, we obtain

$$\frac{d}{dt}Tc_u(t) = Tc_v(t)$$

$$\frac{d}{dt}Tc_v(t) = TD^{(2)}T^{-1}Tc_u(t) + Tc_f, \quad t > 0$$

using the relations

$$u(t) = Tc_u(t)$$

$$f = Tc_f = \left\{\left(P_{\tilde{V}_J}f\right)(x_l)\right\}_{l=0}^{2^J-1};$$

$$D^{(2)} = TD^{(2)}T^{-1};$$

we find

$$\frac{d}{dt}u(t) = v(t) \tag{4.35}$$

$$\frac{d}{dt}v(t) = D^{(2)}u(t) + f, \quad t > 0 \tag{4.36}$$

with the initial condition

$$u(0) = h = \left\{\left(P_{\tilde{V}_J}h\right)(x_l)\right\}_{l=0}^{2^J-1};$$

$$v(0) = g = \left\{\left(P_{\tilde{V}_J}g\right)(x_l)\right\}_{l=0}^{2^J-1}.$$

4.8.9 Hybrid Representation

Multiplying (4.35) from the left with W, we obtain

$$\frac{d}{dt}\breve{u}(t) = \breve{v}(t) \tag{4.37}$$

$$\frac{d}{dt}\breve{v}(t) = \breve{D}^{(2)}\breve{u}(t) + \breve{f}, t > 0 \tag{4.38}$$

with initial condition

$$\breve{u}(0) = Wh;$$
$$\breve{v}(0) = Wg.$$

4.8.10 Results and Discussion

For the test problem, we take $J = 6$, $\delta = 0.005$, $\lambda = 3$, $D = 8$, and

$$f(x) = e^{-t}\sin(2\pi x) - (2\pi)^2 e^{-t}\sin(2\pi x).$$

The initial conditions are

$$u(x, 0) = \sin(2\pi x)$$
$$u_t(x, 0) = -\sin(2\pi x)$$

Thus, the exact solution is $u = e^{-t}\sin(2\pi x)$. We then compare the results with the exact solution $u(x) = e^{-t}\sin(2\pi x)$ and then we compute the error using all the four methods mentioned above. Define

$$\|u\|_\infty = \max_{0\le x<1} |u(x)|$$

$$\|u\|_{J,\infty} = \max_{k=0,1,\cdots,2^J-1} |u(\frac{k}{2^j})|.$$

Table 4.2 illustrate the relative error obtained when the wave equation is solved in the Physical Space for different values:

In Table 4.2, we have discussed the dependence of the error $\|u - u_j\|_{J,\infty}$ on J, D. More precisely,

$$\|u - u_j\|_{J,\infty} = O(2^{-J(D-2)})$$

and

$$\|u - u_j\|_\infty = O(2^{-JD/2}).$$

The high convergence observed in the table means that the solution $u(x)$ is approximated to D^{th} order in the norm $\|.\|_{J,\infty}$ even though the subspace $\tilde{V}_J$ can only represent exactly polynomials upto degree $D/2 - 1$. This phenomenon is known as super convergence result.

J	$D = 6$	$D = 8$
2	0.6490	0.6345
3	0.5444	0.5868
4	0.5201	0.5243
5	0.4871	0.4900
6	0.4520	0.4675

Table 4.2: **The relative error shows the different values of J and D.**

4.8.11 Conclusion

Figures 4.1 to 4.10 compares the exact solution and computed solutions using scaling functions, physical space, and wavelet space. Using scaling functions, the solution dies down as time increases. But using wavelets, the solution dies down faster as time increases. In case of physical space, the solution dies down slightly faster than that in the case of scaling functions as time increases.

4.9 Wavelet-Galerkin Method for Regularized Long Wave Equation

We use the Wavelet-Galerkin method to solve the $1D$ regularized long wave (RLW) equation. Let $I = (0, 1)$ be a bounded open interval. We consider the following regularized long wave (RlW) equation

$$u_t - \gamma u_{xxt} + \alpha u u_x = f(x); \quad x \in I, \quad t > 0 \tag{4.39}$$

$$I.C.: \quad u(x, 0) = u_0(x),$$

$$B.C.: \quad u(0, t) = u(1, t) = 0; \quad x \in I, t > 0$$

where u represents the amplitude of the wave with respect to the level of undisturbed fluid, α is a positive constants, and u_0 and f are given functions. The above equation was first introduced by Peregrine to describe the behavior of the unmodular bore. It also arises in the study of water waves and in acoustic plasma waves. Since analytical solution is difficult to obtain, one resorts to numerical methods. Earlier the RLW equation has been solved numerically using finite difference methods, finite element method and also mixed finite element method. In this section, we have made an attempt to solve the RLW equation using Wavelet-Galerkin method and the corresponding error estimates.

Let $V = H_0^1(I)$ where

$$H_0^1(I) = \{v \in H^1(I) : v(0) = v(1) = 0\}.$$

The weak formulation of (4.39), is to find $u(\cdot, t) \in H_0^1$ such that

$$(u_t, v) + \gamma(u_{xt}, v_x) + \alpha(uu_x, v) = (f, v), v \in H_0^1 \tag{4.40}$$

$$u(0) = u_0$$

Let V_j be a finite dimensional subspace of $H_0^1(I)$ and let $P_J : H_0^1 \to V_J$ be the orthogonal projection. Then P_J satisfies for $v \in H^r(I) \cap H_0^1$

$$\|v - P_J v\| + 2^{-j}\|v - P_J v\|_1 \leq C2^{-Jr}\|v\|_r.$$

Further

$$\|v - P_J v\|_{L^\infty} + 2^{-j}\|v - P_J v\|_{W^{1,\infty}} \leq C2^{-Jr}\|v\|_{W^{r,\infty}}.$$

4.9.1 Semi-discrete Wavelet-Galerkin Method

In semi-discrete Galerkin approximation, we seek $u_J(t) \in V_J$ such that

$$(u_{Jt}, \chi) + \gamma(u_{Jxt}, \chi_x) + \alpha(u_J u_{Jx}, \chi) = (f, \chi), \tag{4.41}$$

where $\chi \in V_J$ and

$$u_J(0) = u_{0J}$$

where u_{0J} is a suitable approximation of u_0 onto V_J. Since V_j is finite dimensional subspace of H_0^1, (4.41) leads to a system of nonlinear ODE's. By an application of Picard's estimates, (4.41) has a unique solution in a neighborhood of $(0, t_j)$. To continue the solution beyond t_J, we need the following apriori bounds.

Theorem 4.9.1 *Let u_J be a solution of (4.41). Then the following apriori bounds holds*

$$\|u_J(t)\|_1 \leq C(\gamma)\left(\|u_J(0)\|_1 + \int_0^t \|f(s)\|ds\right)$$

and

$$\|u_J(t)\|_\infty \leq C(\gamma)\left(\|u_J(0)\|_1 + \int_0^t \|f(s)\|ds\right).$$

Proof: The proof is on the same line as given in Section 4.8.

4.9.2 Error Analysis for the Semi-discrete Scheme

A direct comparison between u and u_J does not yield optimal order of convergence. Therefore, we need to introduce an auxiliary function $\tilde{u}_J \in V_J$ which is defined by

$$a(u_x - \tilde{u}_J x, \chi_x) = 0, \chi \in V_J \tag{4.42}$$

Let $u - \tilde{u}_J = \eta$. Then the following estimates hold:

Lemma 4.9.2

$$\|\eta\|_{L^2} + 2^{-J}\|\eta\|_1 \leq C2^{-Jr}\|u\|_r,$$

and

$$\sum_{i=0}^{2}\left(\left\|\frac{\partial^i \eta}{\partial t^i}\right\| + 2^J\left\|\frac{\partial^i \eta}{\partial t^i}\right\|_1\right) \leq C2^{-Jr}\sum_{i=0}^{2}\left\|\frac{\partial^i \eta}{\partial t^i}\right\|_r$$

Proof: The proof is on the same line as given in Section 4.8.

Theorem 4.9.3 *With $u_J(0) = P_J u_0$, the following estimate holds*

$$\|e(t)\|_1 \leq C2^{-J(r-1)}(\|u_0\|_r + \|u\|_r + \int_0^t (\|u(s)\|_r + \|u_t(s)\|_{r-1})ds).$$

Proof: The proof is on the same line as given in Section 4.8.

4.9.3 Computational Result for the RLW Equation

We consider now Regularized long wave (RLW) equation. The periodic initial-value problem for a particular form of RLW equation is

$$u_t = \gamma u_{xxt} - \alpha u u_x, t > 0$$

$$u(x,0) = h(x),$$

$$u(x,t) = u(x+1,t), t \geq 0,$$

where γ and α are positive constant and

$$h(x) = h(x+1).$$

This problem is discretized in the same manner as we obtain the system

$$\frac{d}{dt}u(t) = L_u(t) + N(u(t))u(t), \quad t \geq 0$$

$$u(0) = h \equiv [h(x_0, h(x_1), \cdots, h(x_{N-1}))]^T$$

where

$$L = \gamma D^{(2)} - I$$

and

$$N(u(t)) = -diag\,(Du(t))$$

with

$$D = D^{(1)}.$$

We solve the RLW equation using scaling functions, wavelets, hybrid representation and also in the physical space. We have used ODE solvers to solve RLW equation for which we have chosen the values $\gamma = 0.001, \alpha = 1$, and $h(x) = \sin(2\pi x)$. The numerical data are $J = 6, \lambda = 3$, and $D = 8$ and we compare it with the exact solution $u = e^{-t}\sin(2\pi x)$.

4.9.4 Conclusion

Figures 4.11 to 4.20 compares the exact solution and computed solutions using scaling functions, physical space, and wavelet space. Using scaling functions, the solution dies down as time increases. But using wavelets, the solution dies down faster as time increases. In case of physical space, the solution dies down slightly faster than that in the case of scaling functions as time increases. For different values of t and γ, we get the corresponding solutions of RLW equation as shown in the figure. We have seen that as γ is strengthen, the solution dies down faster as time increases. Increment in time and strengthening of γ makes the solution die down faster.

4.10 Wavelet-Galerkin Method for Parabolic Equation

We consider the following parabolic equation:

$$\left.\begin{array}{l} u_t - (a(x)u_x)_x + a_0 u = f(x) \\ u(x,0) = u_0(x) \\ u(0,t) = u(1,t) = 0 \end{array}\right\} x \in [0,1], \quad t \in (0,\infty) \tag{4.43}$$

Assume that $a \geq \alpha_0 > 0$, $a_0 \geq 0, |a|, |a_0| \leq M$, $I = (0,1)$. Let $V = H_0^1(I)$, where

$$H_0^1(I) = \left\{ v \in L^2(I) : \frac{dv}{dx} \in L^2(I), v(0,t) = v(1,t) = 0 \right\},$$

with the norm

$$\|v\|_1 = \left(\|v\|^2 + \|\frac{dv}{dx}\|^2 \right)^{\frac{1}{2}}.$$

The weak formulation of (4.43) is to find $u(\cdot, t) \in V$ such that

$$(u_t, v) + a(u, v) = (f, v), v \in V \tag{4.44}$$

$$(u(0), v) = (u_0, v)$$

where

$$a(u, v) = \int_0^1 (a(x)u'(x)v'(x) + a_0(x)u(x)v(x)).$$

Note that the bilinear form $a(\cdot, \cdot)$ is bounded in the sense that

$$\begin{aligned} |a(u,v)| &\leq \int_0^1 |a(x)||u'(x)||v'(x)|dx + \int_0^1 |a_0(x)||u(x)||v(x)|dx \\ &\leq M\left(\int_0^1 |u'(x)||v'(x)|dx + \int_0^1 |u(x)||v(x)|dx\right) \\ &\leq M\|u\|_1\|\|v\|_1. \end{aligned}$$

In the last step, we have used Holder's inequality. Further, $a(\cdot, \cdot)$ is coercive, that is, there is a constant $\alpha_0 > 0$ such that

$$\begin{aligned} a(u,v) &= \int_0^1 a(x)u'(x)^2dx + \int_0^1 a_0(x)u(x)^2dx \\ &\geq \alpha_0 \int_0^1 |u'(x)|^2 \geq \alpha_0\|u(x)\|. \end{aligned}$$

Here, we have used Poincare's inequality. In a Galerkin type approach, we first introduce a subspace V_J of V satisfying the homogeneous boundary conditions:

$$V_J^0 = \{u \in V_J(0,1)|u(0) = u(1) = 0\}.$$

The semi-discrete Wavelet Galerkin method is to find $u_J(t) \in V_J^0,\ \ t \geq 0$ such that

$$(u_{Jt}, v_J) + a(u_J, v_J) = (f, v_J), \quad v_J \in V_J^0 \tag{4.45}$$

with initial condition

$$(u_0, v_J) = (u_0, v_J).$$

4.10.1 Error Analysis for the Semi-Discrete Method

A direct comparison between u and u_J does not yield optimal order of convergence. Therefore, we need to introduce an auxiliary function $\tilde{u} \in V_J$ which is defined by

$$a(u - \tilde{u}_J, \chi) = 0, \quad \chi \in V_J \tag{4.46}$$

Let $u - \tilde{u}_J = \eta$. Then the following estimates hold:

Lemma 4.10.1

$$\|\eta\| + 2^{-J}\|\eta\|_1 \leq C2^{-Jr}\|u\|_r,$$

and

$$\|\eta_t\| + 2^{-J}\|\eta_t\|_1 \leq C2^{-Jr}\|u_t\|_r,$$

Proof: The proof is same as described in Section 4.8.

Theorem 4.10.2 *With $u_h(0)$ as $\tilde{u}_h(0)$ or P_{Ju_0} , there exist a constant C such that*

$$\|u(t) - u_J(t)\| \leq C2^{-Jr}\left(\|u_0\|_r + \int_0^t \|u_t(s)\|_r ds\right).$$

Proof: The proof is same as described in Section 4.8.

4.10.2 Computational Results

For simplicity of exposition, we consider the periodic initial-value problem for the heat equation

$$u_t = \nu u_{xx} + f(x), \quad t > 0 \tag{4.47}$$

$$u(x, 0) = h(x)$$

$$u(x, t) = u(x + 1, t), \quad t \geq 0; \quad x \in R$$

where ν is a positive constant, $f(x) = f(x+1)$ and $h(x) = h(x+1)$. However, the computational results can be carried out for non periodic problems with general parabolic equations.

4.10.3 Representation with respect to Scaling Functions

For the discretization of (4.47), we replace $u(x)$ with its scaling function approximation as

$$u_J(x,t) = \sum_{k=0}^{D-1} (c_u)_{J,k}(t)\tilde{\phi}_{J,k}(x), \quad J \in N_0. \tag{4.48}$$

From (4.9), we obtain that

$$u''_J(x,t) = \sum_{k=0}^{D-1} (c_u^{(2)})_{J,k}(t)\tilde{\phi}_{J,k}(x); \tag{4.49}$$

where $(c_u^{(2)})_{J,k}$ is given as in (4.11), i.e.

$$(c_u^{(2)})_{J,k}(t) = [D^{(2)}c_u(t)]_k = \sum_{n=2-D}^{D-2} = (c_u)_{J,\langle n+k\rangle_{2^J}}(t)2^{Jd}\nu_n^d, \quad k = 0,1,\cdots,2^J-1;$$

with γ_n^d defined in equation (4.1).

4.10.4 Galerkin Method

Multiplying (4.47) by $\tilde{\phi}_{J,l}(x)$ and integrating over the unit interval, we obtain the relation

$$\int_0^1 u_{Jt}(x,t)\tilde{\phi}_{J,l}(x)dx = \nu \int_0^1 u''_{Jt}(x,t)\tilde{\phi}_{J,l}(x)dx + \int_0^1 f(x)\tilde{\phi}_{J,l}(x)dx.$$

On substituting (4.48) and (4.49) in the above equation, we obtain

$$\int_0^1 \frac{d}{dt}\left(\sum_{k=0}^{D-1}(c_u)_{J,k}(t)\tilde{\phi}_{J,k}(x)\right)\tilde{\phi}_{J,l}(x)dx = \nu\int_0^1 \sum_{k=0}^{D-1}(c_u^2)_{J,k}(t)\tilde{\phi}_{J,k}(x)\tilde{\phi}_{J,l}(x)dx + \int_0^1 f(x)\tilde{\phi}_{J,l}(x)dx.$$

By orthonormality of the periodized scaling functions, we obtain

$$\frac{d}{dt}(c_u)_{J,l}(t) = \nu(c_u^{(2)})_{J,l}(t) + (c_f)_{J,l}, \quad l = 0,1,\cdots,2^J-1,$$

where

$$(c_f)_{J,l} = \int_0^1 f(x)\tilde{\phi}_{J,l}(x)dx.$$

In vector notation, this becomes

$$\frac{d}{dt}c_u(t) = \nu c_u^{(2)}(t) + c_f,$$

and using (4.13), we obtain the linear system of equations

$$\frac{d}{dt}c_u(t) = \nu D^{(2)}c_u(t) + c_f, \quad t > 0 \tag{4.50}$$

$$c_u(0) = c_h$$

where c_h is given by,

$$(c_h)_{J,k} = \int_0^1 h(x)\tilde{\phi}_{J,k}(x)dx, \quad k = 0, 1, \cdots, 2^J - 1.$$

Equation (4.13) represent the scaling function discretization of (4.47). Hence, this method belongs to class 1 as described earlier.

4.10.5 Representation with respect to Wavelets

Multiplying (4.50) from the left by W and inserting the identity $W^T W = I$ yields

$$\frac{d}{dt}Wc_u(t) = \nu W D^{(2)} W^T W c_u(t) + W c_f, \quad t > 0.$$

Using the relations

$$d_u = Wc_u \tag{4.51}$$

$$d_f = Wc_f \tag{4.52}$$

yields

$$\breve{D}^{(2)} = W D^{(2)} W^T$$

we then obtain

$$\frac{d}{dt}d_u(t) = \nu \breve{D}^{(2)} d_u(t) + d_f, \quad t > 0 \tag{4.53}$$

with the initial condition

$$d_u(0) = Wc_h.$$

4.10.6 Representation with respect to Physical Space

Multiplying (4.50) from the left by T and proceeding as above, we obtain

$$\frac{d}{dt}Tc_u(t) = TD^{(2)}T^{-1}Tc_u(t) + Tc_f, \quad t > 0.$$

Using the relations

$$u(t) = Tc_u(t)$$

$$f = Tc_f = \{\left(P_{\check{V}_J}\right)(f)(x_l)\}_{l=0}^{2^J-1}$$

and

$$D^{(2)} = TD^{(2)}T^{-1},$$

we find that

$$\frac{d}{dt}u(t) = \nu D^{(2)}u(t) + f, \quad t > 0 \tag{4.54}$$

with the initial condition

$$u(0) = h = \{\left(P_{\check{V}_J}h\right)(x_l)\}_{l=0}^{2^J-1}.$$

4.10.7 Hybrid Representation

In this subsection, we mention a second possibility for discretizing (4.47) using wavelets. This is essentially a combination of the approaches that lead to (4.53) and (4.54), and we proceed as follows:

Multiplying (4.54) from the left by W and using the identity $W^TW = I$, we obtain

$$\frac{d}{dt}W_u(t) = \nu WD^{(2)}W^TW_u(t) + Wf, \quad t > 0.$$

Defining the wavelet transformed vectors as

$$\check{f} = Wf \quad and \quad \check{u} = Wu,$$

we find that

$$\frac{d}{dt}\check{u}(t) = \nu\check{D}^{(2)}\check{u}(t) + \check{f}, \quad t > 0,$$

with the initial condition

$$\check{u}(0) = Wh,$$

where $\check{D}^{(2)}$ is the same as in (4.19). This approach by passes the scaling coefficient representation and relies on the fact that the FWT can be applied directly to function values of f. As the elements in $\check{u}$ will behave similarly as the true wavelet coefficients $\check{d}$. Therefore, wavelet compression is as likely in this case as with the pure wavelet representation (4.53). Hence, this method belongs to Class 2 as described earlier.

4.10.8 Conclusion

For the test problem, we take $J = 6$, $\Delta t = 0.005$, $0 \leq t \leq 2$, $\lambda = 3$, $D = 8$, $\nu = 0.01/\pi$, $f = (\nu 4\pi^2 - 1)e^{-t}\sin(2\pi x)$. Thus, the exact solution is $u = \exp -t\sin(2\pi x)$. Figures 4.27 to 4.37 compares the exact solution and computed solutions using scaling functions, physical space, wavelet space, and hybrid space. Using scaling functions, the solution dies down as time increases. But using wavelets, the solution dies down faster as time increases. In case of physical space, the solution dies down slightly faster than that in the case of scaling functions as time increases. Table 4.3 illustrate the relative error obtained when the heat equation is solved in the Physical Space for different values:

J	$D = 6$	$D = 8$
2	0.0198	0.0063
3	0.0022	2.20 e - 4
4	1.753 e - 4	3.84 e - 5
5	3.74 e -5	2.91 e - 5
6	3.90 e -5	3.92 e - 5

Table 4.3: **The relative error shows the different values of J and D.**

In Table 4.3, we have discussed the dependence of the error $\|u - u_j\|_{J,\infty}$ on J, D in the physical space. The convergence rate is as follows:

$$\|u - u_j\|_{J,\infty} = O(2^{-J(D-2)})$$

and

$$\|u - u_j\|_{\infty} = O(2^{-JD/2}).$$

4.11 Wavelet-Galerkin Method for Burger's Equation

In this section, we shall discussed the Wavelet-Galerkin method for the Burger's equation.

$$\left.\begin{aligned} u_t + uu_x = \nu u_{xx} + f, 0 < x < 1,\ \ t > 0, \\ u(x,0) = u_0(x);\ \ 0 < x < 1, \\ u(x+1,t) = u(x,t);\ \ 0 < x < 1. \end{aligned}\right\} \tag{4.55}$$

Burger's equation describe the evolution of the field $u = u(x,t)$ under non-linear advection and linear dissipation. When the viscosity μ is null, the field will develop a shock in a time. For small viscosity the solution will be slightly smoothed version of inviscid (shock) solution. That is sharp gradients will develop and slowly dissipates as $t \to \infty$ and the solution decays to zero. For moderate values of the viscosity, the solution decays to zero and gradients do not intensify (see [?]). Burger's equation is a useful test case for numerical methods due to its simplicity and predictable dynamics. The challenge is to resolve the sharp gradients/shocks that occur at small and vanishing viscosity and accurately track their revolution. In this section, we assume periodic boundary conditions.

A useful property of Burger's equation is that for certain values of time and viscosity the exact solution can be generated numerically using Cole-Hopf transformation. This makes it possible to compare the accuracy of different numerical methods by comparing them with exact solutions.

The Wavelet-Galerkin method stably represent the solutions to Burger's equation for small, and even vanishing viscosity. The oscillations associated with Gibb's phenomenon at a shock are confined to the viscinity of the shock and are smaller than those that arise in McCormac finite difference approximations. Even for quite small viscosity, the oscillations stabilize and decay to the correct solution. The Wavelet-Galerkin method may provide a uniform, no-problem-specific technique for shock capture and more generally, for resolving solutions with localized and sharp gradients.

Wavelet methods are expected to perform well on Burger's equation because the wavelet basis can decouple the localized details of the solution from its underlying globally smooth behaviour. There is hardly any result on convergence analysis. A priori estimates for equation (4.55) can be discussed in the same way as we have discussed in the case of hyperbolic PDE and parabolic PDE.

4.11.1 Computational Results

We consider

$$\left.\begin{aligned} u_t + uu_x = \nu u_{xx} - (u_\rho)u_x, \ \ t > 0, \\ u(x,0) = h(x), \\ u(x,t) = u(x+1,t), \quad t \geq 0 \end{aligned}\right\} x \in \mathbf{R} \tag{4.56}$$

where μ is a positive constant, $\rho \in \mathbf{R}$, and $h(x) = h(x+1)$. The wavelet discretization use the following system of odes.

$$\frac{d}{dt}u(t) = Mu(t) + s\left(u(t)\right)u(t)$$

$$u(0) = \left[h(x_0), h(x_1), h(x_2), \ldots\ldots, h(x_{N-1})\right]^T$$

where

$$M = \nu D^{(2)} - \rho I; \; and \;\; s\left(u(t)\right) = -diag\left(Du(t)\right); \;\; withD = D^{(1)}$$

where D^2 wavelet differentiation matrix.

4.11.2 Results and Discussion

We have used ODE solvers to solve this equation for which we have chosen $u_0(x) = exp\left(\frac{-1}{1-x^2}\right)$. The numerical data are $J = 10$, $D = 8$, $\lambda = 3$, $\epsilon_m = 10^{-11}$, $\epsilon_\nu = 10^{-10}$, $\Delta t = 0.005$, and $n_1 = 100$. We have provide the figures from 4.38 to 4.41 showing the behavior of the solution in physical space and wavelet space for various values of ν at different time levels.

We conclude with the following points:

- The wavelet-Galerkin method appears to be stable for all viscosities including zero.
- The wavelet-Galerkin solution is close to the Exact solution even for small viscosities.
- The time of appearance of shock increases as we strengthen the viscosity.

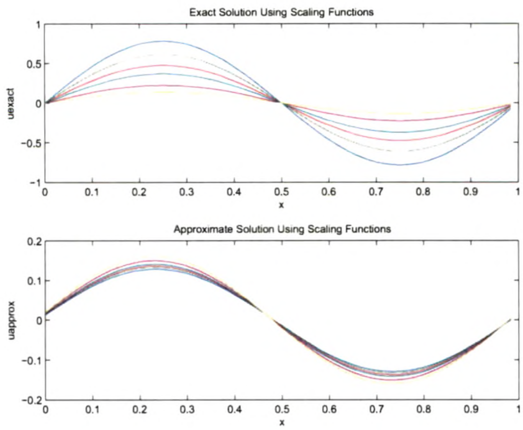

Figure 4.1: **Solution of Wave equation for scaling function representation**

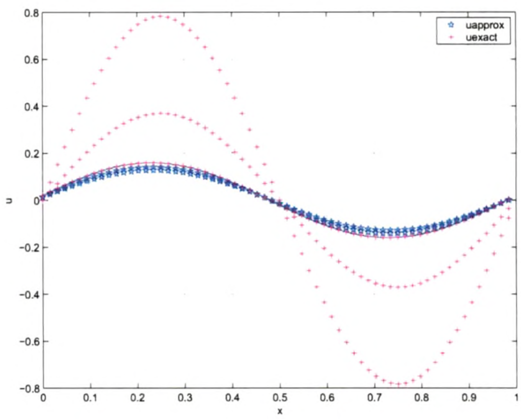

Figure 4.2: **Solution of Wave equation for scaling function representation**

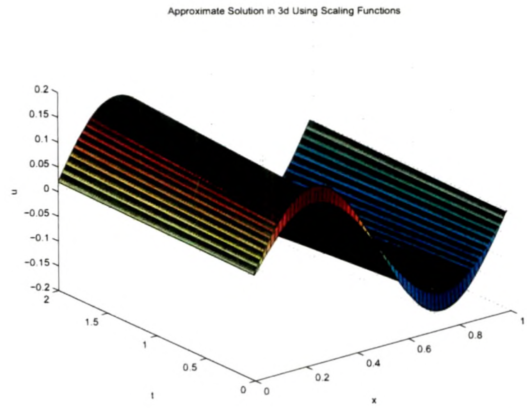

Figure 4.3: **Solution of Wave equation for scaling function representation**

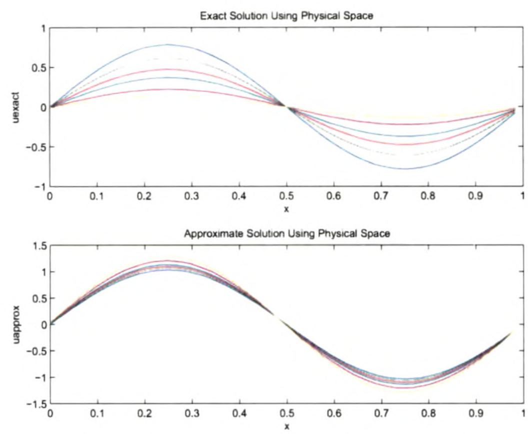

Figure 4.4: **Solution of Wave equation with respect to physical spaces**

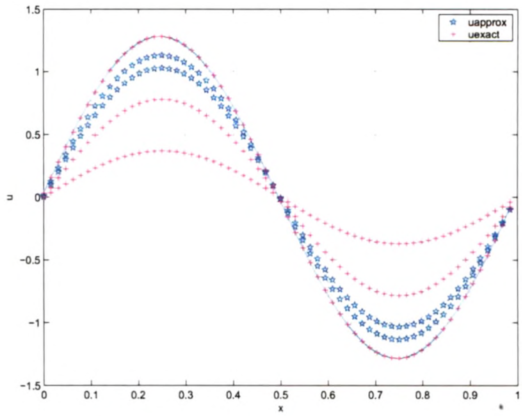

Figure 4.5: **Solution of Wave equation with respect to physical spaces**

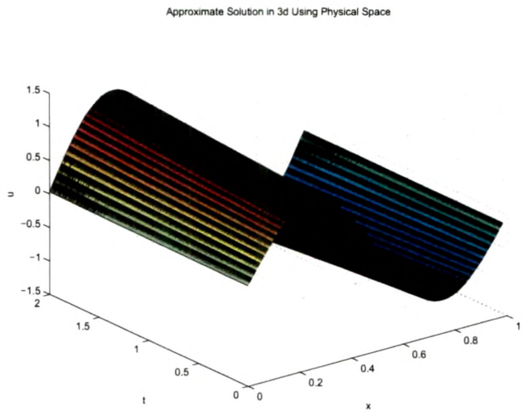

Figure 4.6: **Solution of Wave equation with respect to physical spaces**

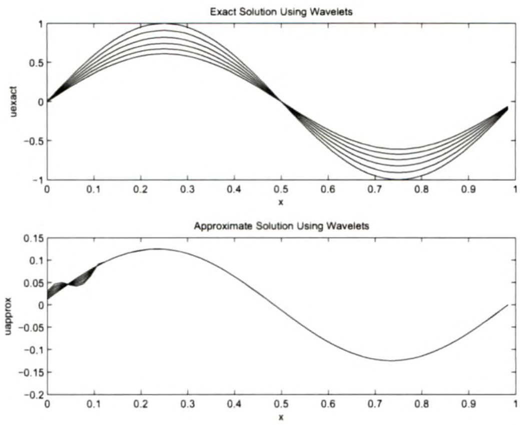

Figure 4.7: **Solution of Wave equation with respect to wavelet spaces**

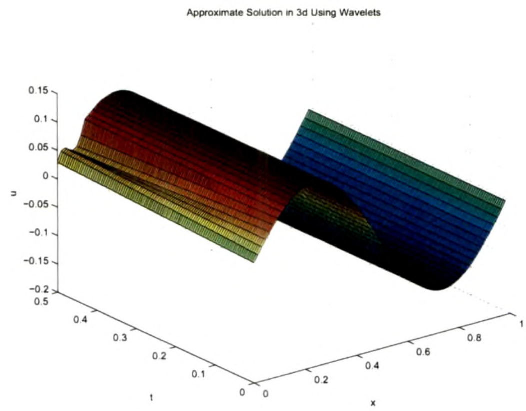

Figure 4.8: **Solution of Wave equation with respect to wavelet spaces**

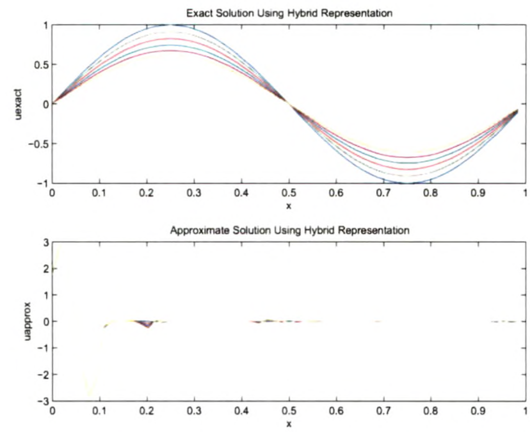

Figure 4.9: **Solution of Wave equation with respect to hybrid spaces**

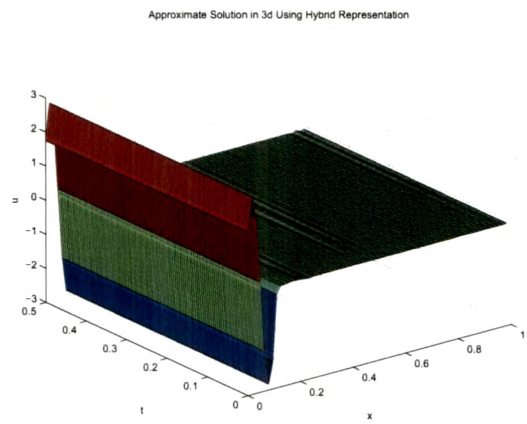

Figure 4.10: **Solution of Wave equation with respect to hybrid spaces**

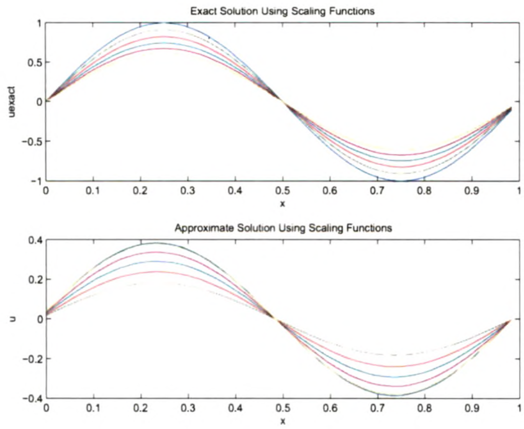

Figure 4.11: **Solution of Regularized Long Wave equation for scaling function representation with** $\gamma = 0.001$

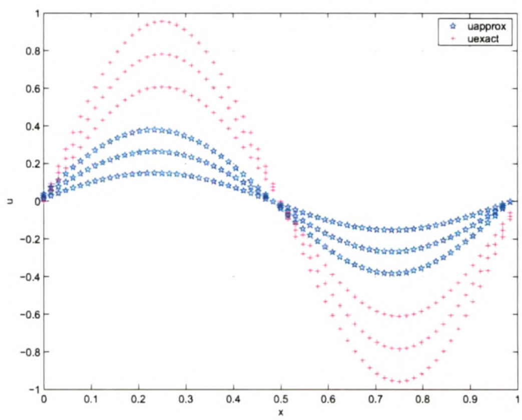

Figure 4.12: **Solution of Regularized Long Wave equation for scaling function representation with** $\gamma = 0.001$

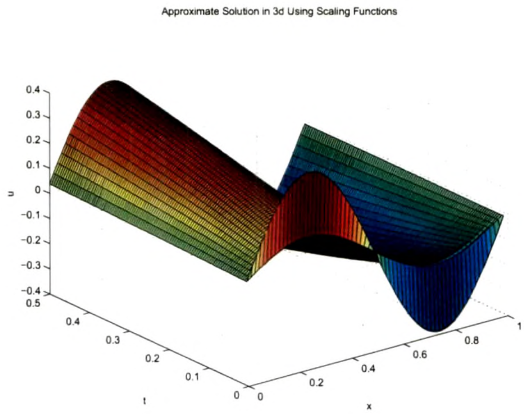

Figure 4.13: **Solution of Regularized Long Wave equation for scaling function representation with** $\gamma = 0.001$

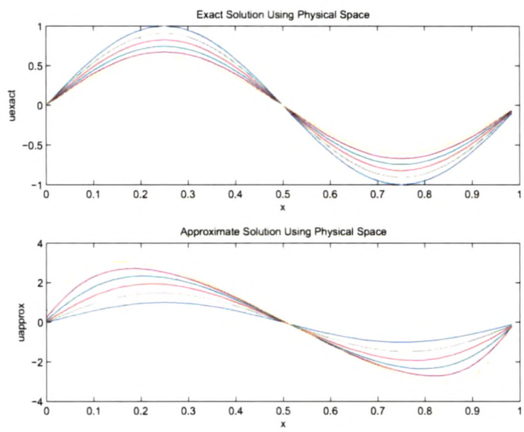

Figure 4.14: **Solution of Regularized Long Wave equation for physical space with** $\gamma = 0.001$

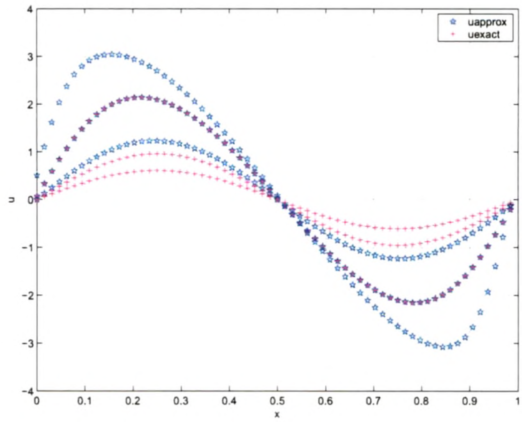

Figure 4.15: **Solution of Regularized Long Wave equation for physical space with** $\gamma = 0.001$

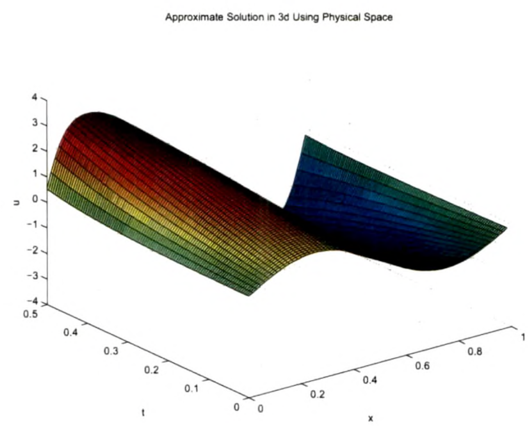

Figure 4.16: **Solution of Regularized Long Wave equation for physical space with** $\gamma = 0.001$

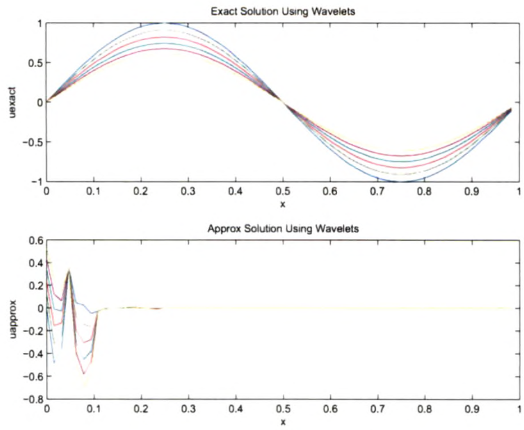

Figure 4.17: **Solution of Regularized Long Wave equation for wavelet space with $\gamma = 0.001$**

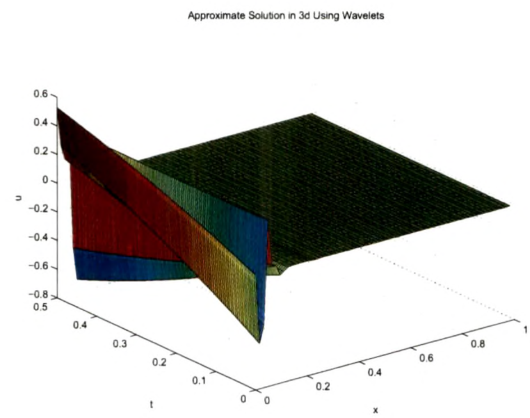

Figure 4.18: **Solution of Regularized Long Wave equation for wavelet space with $\gamma = 0.001$**

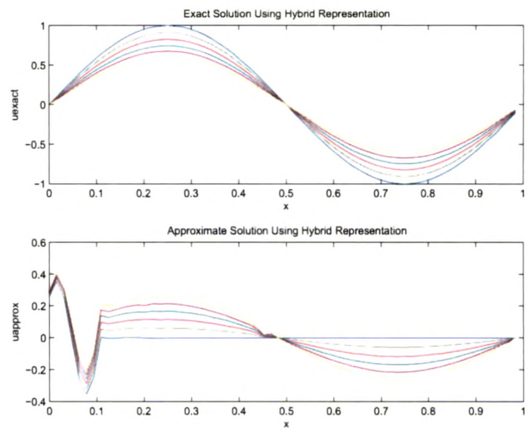

Figure 4.19: **Solution of Regularized Long Wave equation for hybrid space with** $\gamma = 0.001$

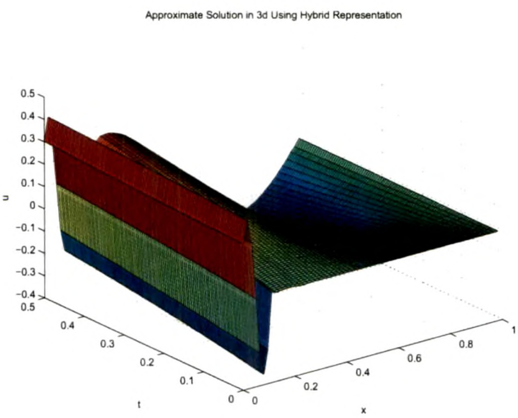

Figure 4.20: **Solution of Regularized Long Wave equation for hybrid space with** $\gamma = 0.001$

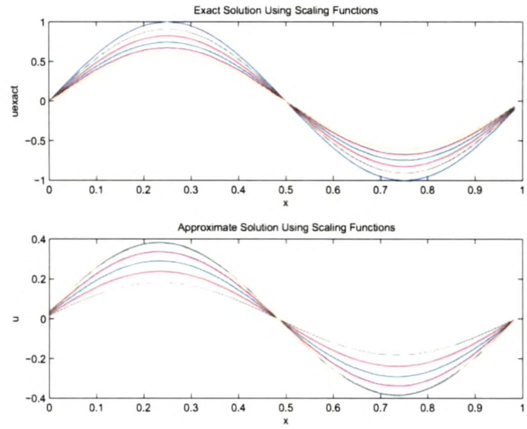

Figure 4.21: **Solution of Regularized Long Wave equation for scaling function with** $\gamma = 0.0001$

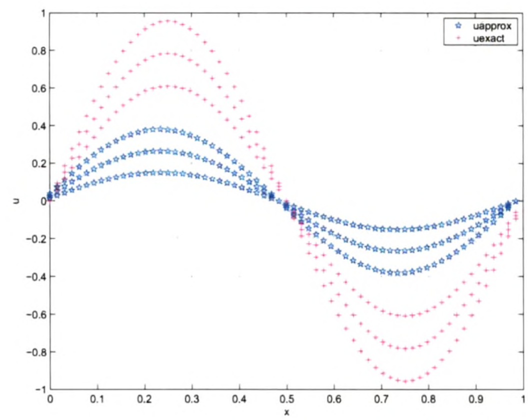

Figure 4.22: **Solution of Regularized Long Wave equation for scaling function with** $\gamma = 0.0001$

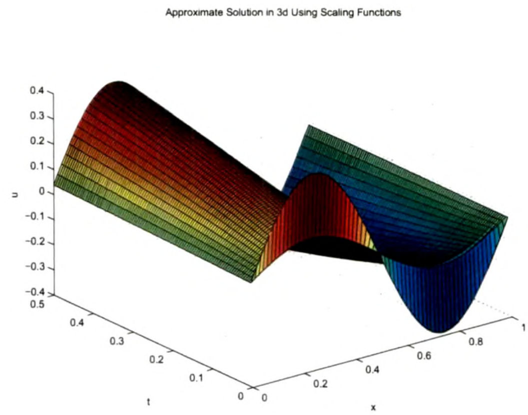

Figure 4.23: **Solution of Regularized Long Wave equation for scaling function with** $\gamma = 0.0001$

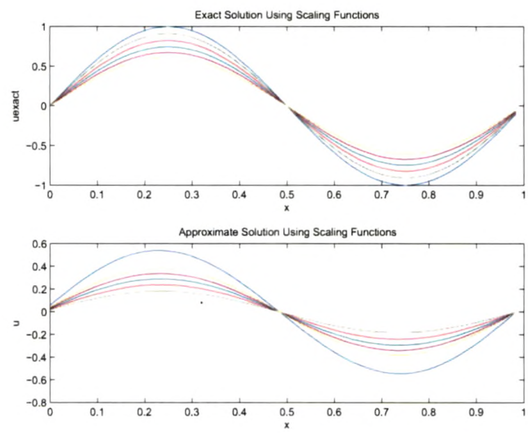

Figure 4.24: **Solution of Regularized Long Wave equation for scaling function with** $\gamma = 0.0001$

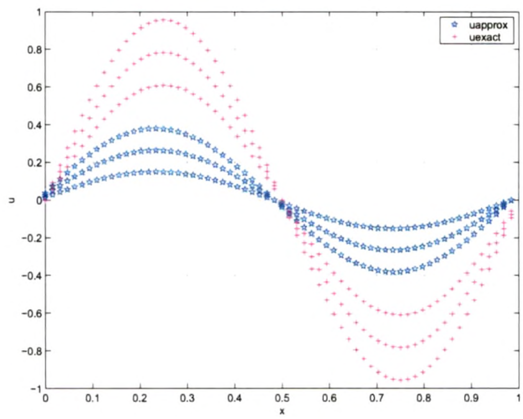

Figure 4.25: **Solution of Regularized Long Wave equation for scaling function with** $\gamma = 0.0001$

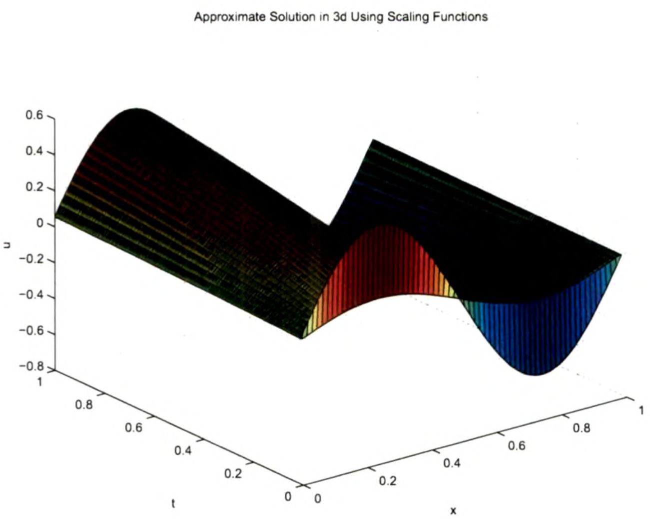

Figure 4.26: **Solution of Regularized Long Wave equation for scaling function with** $\gamma = 0.0001$

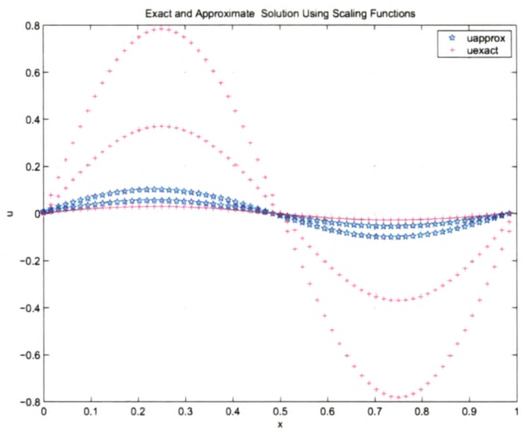

Figure 4.27: **Solution of heat equation for scaling function representation**

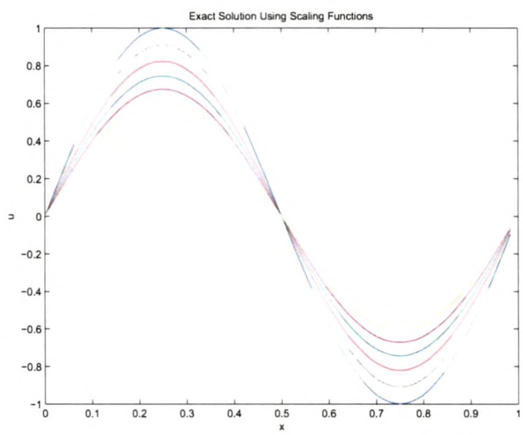

Figure 4.28: **Solution of heat equation for scaling function representation**

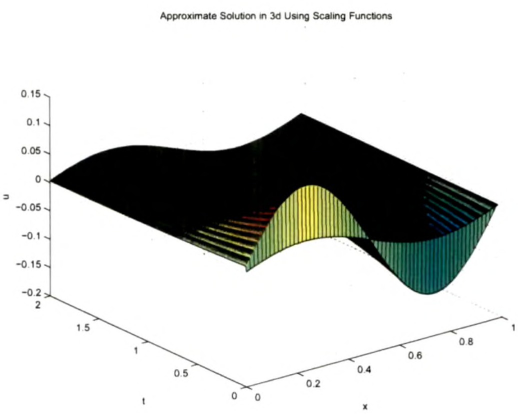

Figure 4.29: **Solution of heat equation for scaling function representation**

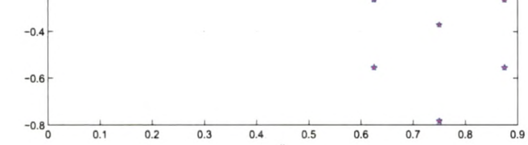

Figure 4.30: **Solution of heat equation for physical space**

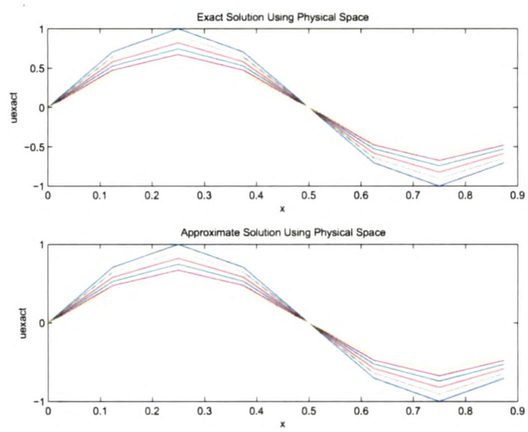

Figure 4.31: **Solution of heat equation for physical space**

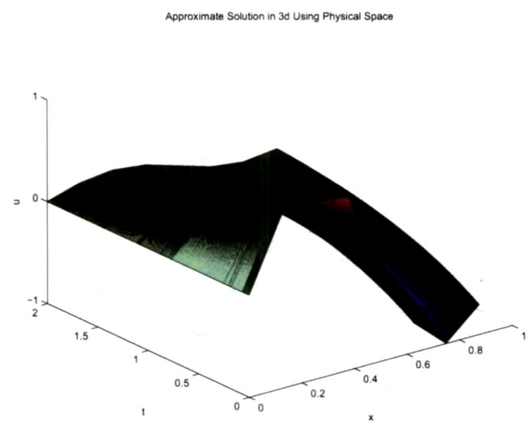

Figure 4.32: **Solution of heat equation for physical space**

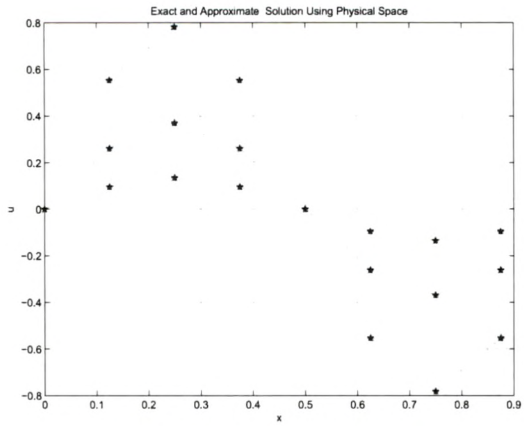

Figure 4.33: **Solution of heat equation for wavelet space**

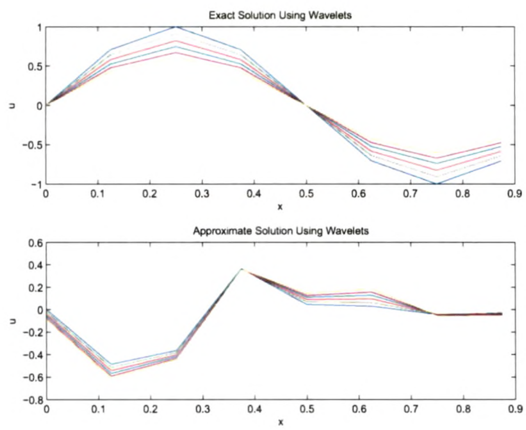

Figure 4.34: **Solution of heat equation for wavelet space**

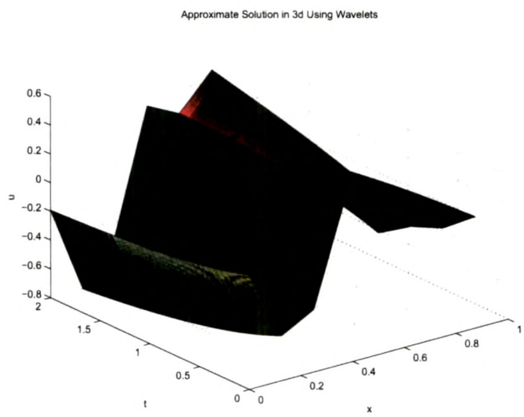

Figure 4.35: **Solution of heat equation for wavelet space**

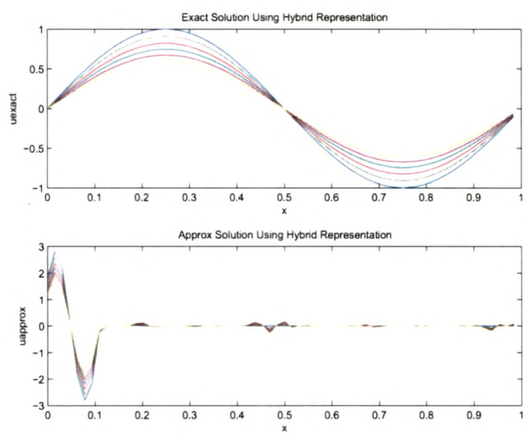

Figure 4.36: **Solution of heat equation for hybrid space**

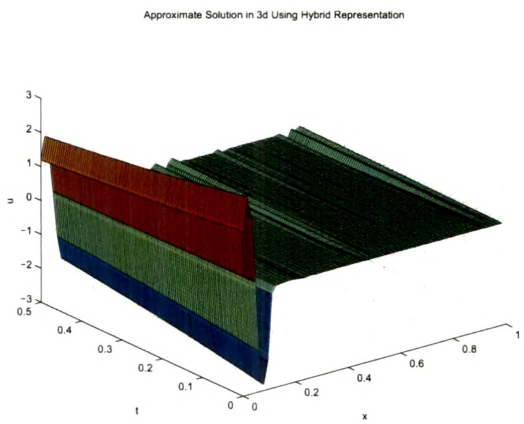

Figure 4.37: Solution of heat equation for hybrid space

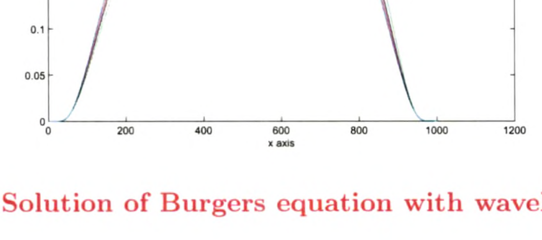

Figure 4.38: Solution of Burgers equation with wavelet method

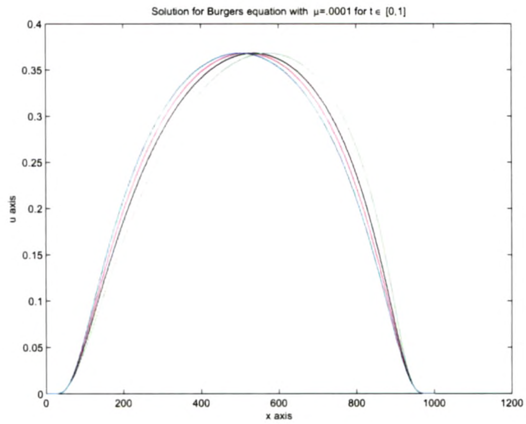

Figure 4.39: **Solution of Burgers equation with wavelet method**

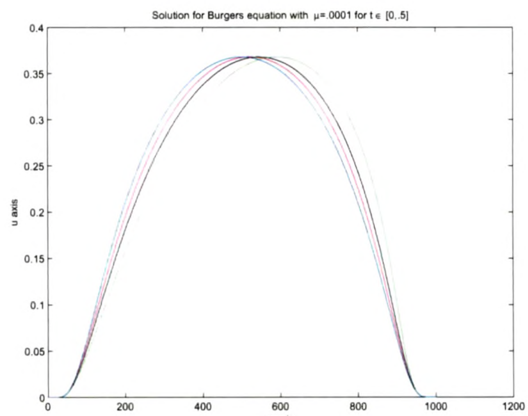

Figure 4.40: **Solution of Burgers equation with wavelet method**

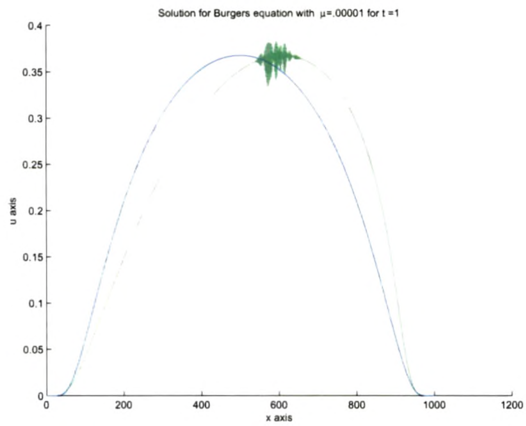

Figure 4.41: **Solution of Burgers equation with wavelet method in which shock appear**